ISSN: 3033-3652

Journal of Physical Mathematics & its Applications

Research Article

Open Access

The 12 Principles of Fluid Dynamics in Closed Conduits Aerodynamic Analysis of a Golf Ball in Flight

Hubert M Quinn

The Wrangler Group LLC, 40 Nottinghill Road, Brighton, Ma. 02135, USA

ABSTRACT

In the real world, fluid flow in closed conduits manifests in both empty conduits, i.e., conduits devoid of solid obstacles and conduits packed with solid particles. The majority of packed beds reported in the literature over the last 100 years, approximately, contain spheroidal particles, for the most part. However, the particles within the packed conduits can vary over a very broad range of shapes and diameter values and when coupled with a wide choice of both conduits and available fluids, this ensemble of experimental variables complicates the study matter, immensely. Empirical studies covering this very broad dynamic range of choices has created many difficulties which has, unfortunately, contributed to a compromised data base of published results. In fact, it is not an exaggeration to suggest that more than 50% of published articles in this field are fraught with errors, misinformation and contradictions. For instance, the use of gases as the fluid of choice, in any experiment, always presents a problem because it is a compressible fluid which means that its' density varies as a function of pressure drop. In addition, because the viscosity also varies with density, the turbulent tipping point of the packed conduit under study cannot be predicted a priori which means that when a compressible fluid is chosen as the fluid of choice in permeability studies, all fluid variables must be measured simultaneously, i.e., viscosity, density, pressure drop and velocity. This is a significant experimentation undertaking for any particular study which many times in the published literature is omitted from the experimental protocol. There is the added difficulty of managing pressure drop, since small particles render large pressure drops while large particles render small pressure drops. If one also considers the additional important variables of packed bed porosity and boundary layer (wall-effects), it becomes very clear that such empirical studies are anything but simple experiments. In fact, there are a total of seven discrete variables and one universal constant embedded in the validated mathematical expression for the pressure flow relationship of packed conduits. A dimpled golf ball, therefore, is a very interesting candidate as a choice for the study of packed beds because it is large in diameter, has a roughened surface, and its' aerodynamic flight takes place through a compressible fluid medium (air), which stands at standard temperature and pressure (STP) in the path of the golf ball flight. Accordingly, a commercial golf ball represents an ideal study candidate and, therefore, the gold standard candidate, albeit of the most difficult variety from an empirical standpoint, to evaluate the performance claims of any fluid flow model which purports to describe the hydrodynamics of packed conduits. In this paper, a relatively new fluid flow model (QFFM) will be used to do exactly that. The aerodynamics of a golf ball in flight will be documented by taking measurements using water, an incompressible fluid, in a packed conduit containing many golf balls, something that has never been accomplished, as far as we know. The teaching of this unique fluid flow model will be used to demonstrate an experimental technique which circumvents/ solves many of the aforementioned issues for studies in packed beds. In short, this paper defines the gold standard of how an experimental protocol should be carried out for permeability in closed conduits, even when the particles are irregular (non- spherical) in shape, compressible (non-rigid), very small in diameter and/or have a roughened surface morphology and, even when the fluid of choice is compressible, such as air.

***Corresponding author**

Hubert M Quinn, The Wrangler Group LLC, 40 Nottinghill Road, Brighton, Ma. 02135, USA.

Received: May 01, 2026; **Accepted:** May 06, 2026; **Published:** May 14, 2026

Introduction

Beginning with the work of Darcy in packed conduits circa 1856 and continuing to this very day, extraordinary amounts of energy have been expended by authors of scientific publications in an attempt to shed light on an understanding of underlying contributions to permeability, not only in packed conduits, but also in empty conduits [1]. Azevedo et al focused their attention on turbulent flow of water in corrugated pipes [2]. Baker et al studied the flow of air through packed conduits containing spherical particles [3]. Erdim et al studied the pressure drop-flow rate correlation of spherical powdered metal particles in packed conduits [4]. Dukhan et al, studied pressure drop in porous media with an eye to reconciliation with classical empirical equations [5]. Anspach et al reported results relating to very high pressure drops in very narrow id HPLC columns using small fully porous particles [6]. Zhong et al. studied air flow through sintered metal particles in the context of the Ergun flow model [7]. Tian et al reported experimental results with sintered ore particles in packed conduits [8]. Mayerhofer et al studied the permeability of irregularly shaped wood particles [9]. Pesic et al studied the effect of temperature on permeability of packed conduits containing spherical particles [10]. Abidzaid et al discusses water flow through packed beds in light of some modified equations [11]. Mirmanto et al studied friction factor of water in micro channels [12]. Capinlioglu et al focused his work on simplified correlations of packed bed pressure drops [13]. Yang et al made comparisons of superficially porous particles in packed HPLC columns [14]. Lundstrom et al used sophisticated analysis techniques to evaluate transitional and turbulent flow in packed beds [15]. Sletfjerding et al reported flow experiments with high pressure natural gas in empty pipes [16]. Langeiandsvik et al studied pipeline permeability and capacity [17]. De Stephano et al studied the performance characteristics of small particles in packed conduits for fast HPLC analysis [18]. Pereira reported on expected pressure drops in commercial HPLC columns [19]. Van Lopik et al studied grain size on nonlinear flow behavior [20]. Li et al discussed particle diameter effects in sand columns [21].

More recently, a new fluid flow model based upon first principles of physics has created a new methodology relating to the fluid dynamics in packed conduits which necessitates an updated format for reporting empirical results of permeability in closed conduits [22-24]. In this paper, we document this gold standard methodology of reporting empirical results which leaves no stone unturned and, accordingly, outlines a standardized format which includes all the necessary data to define this complicated matrix of information. Although this fluid model has been extensively validated by classical studies carried out throughout the history of this field of study, the complexity of experimental design and execution necessitates a step-by-step explanation/documentation. These classical studies include the original work of Reynolds circa 1883 in which he published on the TTP (Turbulent Tipping Point) of water flow in a transparent pipe, the seminal work of Nikuradze in which he measured the impact of sand roughness on the inner wall of a water pipe, the pioneering work of Darcy based upon his water tests in sand-filled pipes mentioned above, the work of Giddings in packed beds containing both spherical glass beads and irregularly shaped silica particles, the classic paper in packed beds by Farkas et al in which he measured the permeability of a packed conduit at extremely low values of the Reynolds number, the now famous study in the Princeton Super pipe which involved the flow of a compressible gas at very high Reynolds number through smooth pipes [25-29].

Empirical Protocols

The analysis begins by selecting a commercial golf ball as the particle of choice and water as the fluid of choice. The golf ball has a spherical particle diameter equivalent, d_p, of 4.27 cm. The fluid has an absolute viscosity, h, of 0.01 poise and a density, r_f, of 1 g/mL at STP (standard temperature and pressure). Secondly, a conduit with a diameter, D, of 4.4 cm and two different lengths, L, of 60 and 664 cm, approximately, is selected. This establishes the ratio value of $D/d_p = 1.03$ and a requirement of $n_p = 14$ and 151, which is the number of golf balls required to exactly fill each conduit, respectively. The golf balls sit on top of each other in the conduits with a single point of contact. Thirdly, two end fittings for the conduit capable of retaining the golf balls, yet having sufficiently high porosity values so as not to generate a measurable pressure drop at the measurement points for the packed conduit, are selected. Finally, a 5 horse-power water pump capable of delivering up to 100 psi pressure drop at a very large water flow rate, i.e. (>50 gals/min), is chosen.

The Golf Ball

The spherical particle diameter equivalent of the golf balls chosen is determined by the use of pycnometry which returns accurate values regardless of particle shape. The spherical particle diameter equivalent d_p of each of three types of spherical particles, yellow golf balls, white golf balls and ping-pong balls, is reported. A quantity of each type of ball, n_p, is dropped into the measuring container (pycnometer) which is already filled with water and the displaced water is collected and measured, as shown in Fig. 1, Thus, by knowing the number of balls and the displaced volume, the spherical particle diameter equivalent of each of the category of balls is calculated by using the equation for a perfect sphere as shown in Table 1.

Figure 1: Pycnometer

Table 1

Type	π	n_p	$V_{(disp)}$	$v_{dp\ (Calc)}$	d_p
		no. of balls	Vol. displaced		
	$\frac{22}{7}$			$\frac{V_{(disp)}}{n_p}$	$(6v_{dp}/\pi)^{(1/3)}$
	none	none	mL	mL	cm
Yellow	3.14	100	4,080	40.80	4.271
White	3.14	90	3,680	40.89	4.274
Pinp-Pong	3.14	178	5,980	33.60	4.003

The Fluid

Water was chosen because it is an incompressible fluid under the conditions of the experiments. By maintaining the water at constant temperature (20°C) under atmospheric pressure, the values for absolute viscosity and density were taken from reference text books. i.e., $\eta = 0.01$ poise and rf = 1.0 g/mL. Because water is an incompressible fluid, both these values remain constant throughout the entire set of measurements (1-100 psi).

The Conduit

We chose an aluminum conduit of diameter 4.4 cm. The conduit was extremely rigid having a wall thickness of 0.25 cm insuring that the diameter value remained constant at all pressure drops measured. The diameter of the pipe was chosen so that a reasonable low value for external porosity e0 would be maintained. This is a very important consideration since it determines the pressure drop range and the performance characteristic of the required pump. For the sake of accuracy of the measurement, a reasonably high pressure drop needs to be attained and, accordingly, sufficient flow rate must be available to attain that pressure. These latter constraints both determine the power requirement of the pump. The length of the conduit needs to be long enough to eliminate end effects and of such a length as to facilitate, precisely, the number of balls necessary for a given packed conduit under study. In other words, selecting the correct conduit length eliminates the need for partial balls to fill the conduit. Because this choice of conduit diameter D and spherical particle diameter equivalent d_p ratio,

$D/d_p = 1.03$, there is a measurable wall effect which most fluid flow models cannot accommodate. The QFFM is amongst the very few models, perhaps the only one extant, which is equipped to handle wall effects.

The Measurement Technique

Water is pumped through the packed conduit using the 5 horse power pump-Goulds, Model e-SV 220 volt. The pressure drop at the entrance to the conduit is measured with a calibrated pressure transducer-XMLP100PD250. For each pressure drop recorded, the volumetric flow rate is measured by collecting the effluent water in a container for a fixed period of time which is determined by stop watch. The collected water is then weighed with a calibrated load cell (electronic balance) and the volume determined by using a value of unity for the fluid density.

The Fluid Model (QFFM)

To establish a basis for comparison, the Quinn Fluid Flow Model (QFFM) is used to generate calculated results for selected hypothetical conduits packed with hypothetical golf balls which have five degrees of dimples (sand-equivalent roughness), i.e., k = 0.0 (1a), k = 0.02 (1b), k = 0.2 (1c), k = 2 (1d), k = 20 (1e) where the units of measure are in microns, i.e. sample (1e) has a dimple depth of 20 micron.. These QFFM computed results are shown in Table 1A for the conduit containing $n_p = 14$, i.e., 14 golf balls.

Table 1A

Table 1A															
Sample	η	ρ_f	n_p	p_f	ε_0	d_c	δ	λ	ω	T	t_Q	TTP	TTP	A	B
ID				$\frac{n_p}{n_{pq}}$	$(1-n_p/n_{pq})$	$\frac{d_p}{abs(p_f)}$	$\frac{1}{\varepsilon_0^3}$	$1+W_N$	$\frac{\delta\lambda}{8\pi}$	$\frac{2\pi}{\omega}$	$\frac{\delta\lambda L d_c \varepsilon_f \rho_f}{\eta}$	$\frac{\delta\lambda Re_{m-C}}{C_{Q-C}}$	Re_{m-C}	$\frac{4\pi r_h^3}{3}$	$\frac{\delta\lambda}{2\pi}$
Golf Ball															
HQC	poise	gcm^{-3}	none	none	none	cm	none	none	rad/sec	sec	sec	none	none	none	none
H2O															
1a	0.01	1.00	14	0.6279	0.3721	6.801	19.40	1.031	0.80	8	302,662	1,686	84	268.19	3.18
1b	0.01	1.00	14	0.6279	0.3721	6.801	19.40	1.445	1.12	6	424,197	1,686	60	268.19	4.46
1c	0.01	1.00	14	0.6279	0.3721	6.801	19.40	1.942	1.50	4	570,097	1,686	45	268.19	5.99
1d	0.01	1.00	14	0.6279	0.3721	6.801	19.40	3.011	2.32	3	883,915	1,686	29	268.19	9.29
1e	0.01	1.00	14	0.6279	0.3721	6.801	19.40	5.314	4.10	2	1,559,987	1,686	16	268.19	16.40

Table 1A displays all the relevant hydrodynamic properties. Firstly, we point out that all 5 hypothetical packed conduits have the same values for $p_f = 0.6279$, the particle volume fraction and $e_0 = 0.3721$, the external porosity. Note, also, that the turbulent tipping point (TTP) values which are identical at the value of $C_Q = 1{,}686$ for all 5 conduits, tend to lower values of the modified Reynolds number as the roughness coefficient value increases. This is the underlying reason for dimples on a golf ball. Note, in particular, that each of the 5 packed conduits has a unique value for the Q time-constant t_Q and that, in addition, the values for l, the wall normalization coefficient, increase as a function of the surface roughness. Finally, we point out that the Q-modified Ergun coefficient A = 268.19 is a constant for all 5 conduits, whereas the value for the coefficient B = dl/(2p) is not a constant value and varies as a function of porosity, d, and wall normalization coefficient l.

The Hypothetical Q Channel (HQC)

The fundamental conceptual underpinning of the QFFM is the HQC, $d_c = d_p/abs\,(p_f)$, where d_c represents the diameter of the HQC.

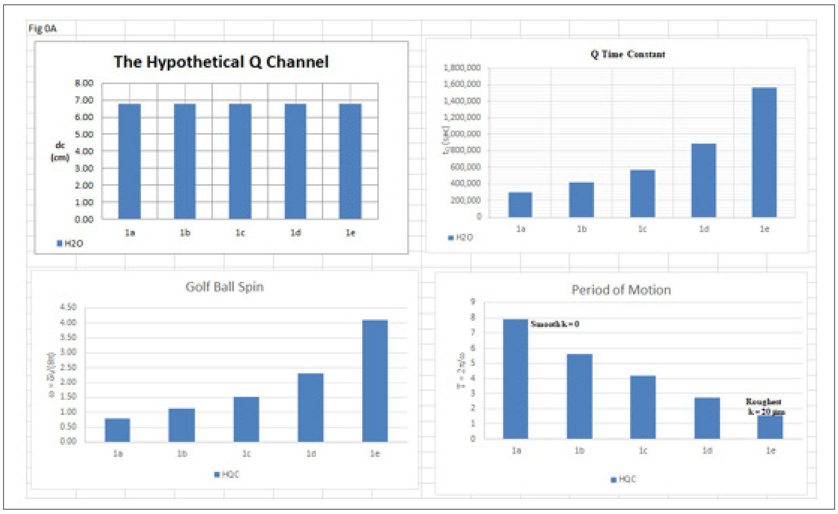

In Figure OA we show that all 5 samples have identical HQC values and that as the roughness coefficient increases, the Q time constant t_Q also increases. We also point out that the golf ball rotation w, in radians/sec. increases as a function of the surface roughness. In contrast, however, the period of the golf ball motion T, in secs, decreases as a function of the surface roughness.

Extrapolation with the QFFM

HQC Extrapolation

Next, we use the QFFM to extrapolate the data for the incompressible fluid water to that for the compressible fluid air. This information is contained in Table 1B.

Table 1B

Sample	η	ρ_f	n_p	p_f	ε_0	d_c	δ	λ	ω	T	t_Q	TTP	TTP	A	B
ID				$\frac{n_p}{n_{pq}}$	$(1-n_p/n_{pq})$	$\frac{d_p}{abs(p_f)}$	$\frac{1}{\varepsilon_0^3}$	$1+W_N$	$\frac{\delta\lambda}{8\pi}$	$\frac{2\pi}{\omega}$	$\frac{\delta\lambda L d_c \varepsilon_f \rho_f}{\eta}$	$\delta\lambda Re_{m\text{-}C}$ $C_{Q\text{-}C}$	$Re_{m\text{-}C}$	$\frac{4\pi r_h^3}{3}$	$\frac{\delta\lambda}{2\pi}$
Golf Ball															
HQC	poise	gcm^{-3}	none	none	none	cm	none	none	rad/sec	sec	sec	none	none	none	none
Table 1B															
Air															
1a	1.83E-04	1.29E-03	14	0.6279	0.3721	6.801	19.40	1.031	0.80	8	21,335	1,686	84	268.19	3.18
1b	1.83E-04	1.29E-03	14	0.6279	0.3721	6.801	19.40	1.446	1.12	6	29,923	1,686	60	268.19	4.46
1c	1.83E-04	1.29E-03	14	0.6279	0.3721	6.801	19.40	1.942	1.50	4	40,187	1,686	45	268.19	5.99
1d	1.83E-04	1.29E-03	14	0.6279	0.3721	6.801	19.40	3.011	2.32	3	62,309	1,686	29	268.19	9.29
1e	1.83E-04	1.29E-03	14	0.6279	0.3721	6.801	19.40	5.314	4.10	2	109,966	1,686	16	268.19	16.40

Note that in Table 1B the fluid is air having an absolute viscosity of 0.000183 poise and a density of 0.00129 g/mL at STP. Note, also, that all the other values in Table 1B, including the values for the HQC, are identical to those in Table 1A except for the parameter t_Q which is significantly smaller. This extrapolation is valid because the Laws of Nature dictate that the hydraulic gradient is a function of the resistance of a given fluid flow embodiment. When that resistance is constant, as it is in any given packed conduit under study, the hydraulic gradient is identical for all fluids, as we will demonstrate below.

Permeability Comparison

In Figure 1A, we show a comparison of permeability measurements in both water and air over a range of pressure drops of 1 to 100 psi.

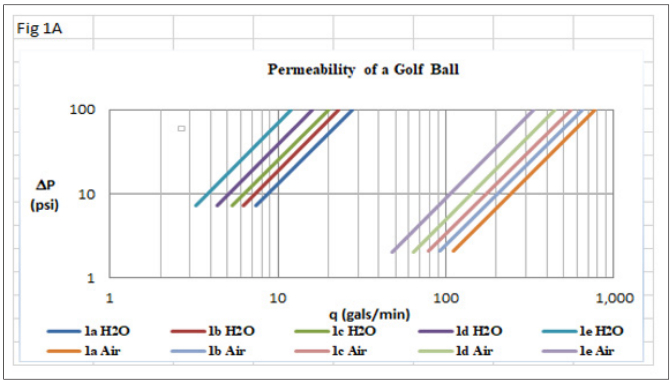

Figure 1A

Note that, as shown in Figure 1A, the flow rates for air are significantly greater than the flow rates in water over the same pressure drop range. Note, also, that the lines are all parallel and have the same slope.

Hydraulic Gradient Comparison

In Figure 2A, we show a comparison of the hydraulic gradient measurements in both water and air overthe same range of pressure drops of 1 to 100 psi.

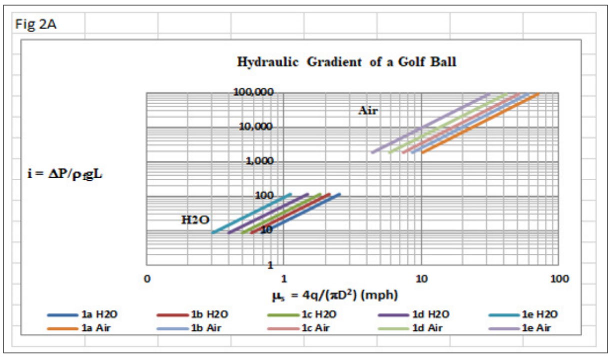

Figure 2A

In Figure 2 A is shown the hydraulic gradient for both water and air. Note that for each sample, the hydraulic gradient is identical in both water and air, the only difference is that the air values are at higher velocities. They are identical since the equation of the line for each sample is identical in air and in water. The fact that the hydraulic gradient is identical in both water and air is the element that establishes the validity of the QFFM to extrapolate from one fluid to another.

A Viscous-Type Friction Factor-the Q-Modified Ergun Equation Comparison

In Figure 3A, we show a comparison of the Q-modified Ergun model in both water and air over the same range of pressure drops of 1 to 100 psi.

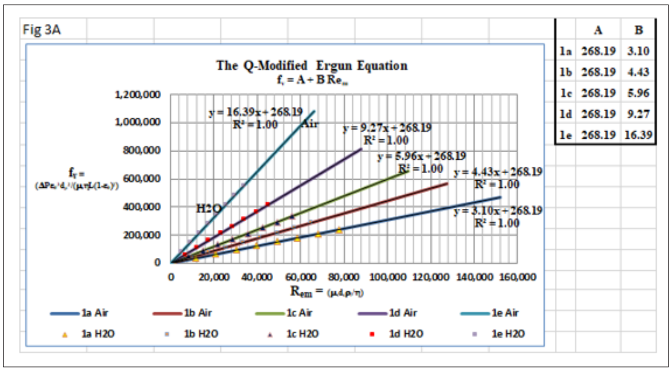

Figure 3A

In Figure 3A is shown the comparison between the Reynolds number values for water and air. Note that the equation of the lines for each conduit is identical for both fluids. Note, also, that the Reynolds number values for air, in the case of each sample, are greater than water. The term on the ordinate of this plot, f_V, is a viscous-type friction factor which means that the measured pressure-drop values for ΔP, are normalized for all the variables in the viscous term which are also measurable, as shown in the formula for f_V shown on the y-axis of the plot. This term is a first level friction factor which produces a linear relationship between f_V and the Reynolds number Re_m when the value of l is constant. Note that for a given packed conduit, this friction factor enables the seamless linear extrapolation from water to air because the equation of the line is identical for both fluids. This is true because the external porosity term, ε_0, and hence the term $\delta = 1/\varepsilon_0^3$, both have a constant value. However, a word of caution is necessary here for two reasons because; (1) the value of the ratio for these 5 conduits is so low at D/dp =1.03, there is a measurable primary wall-effect, i.e., viscous boundary layer; (2) there is, in addition, a secondary wall-effect, i.e., a significant wall roughness coefficient for four of the conduits. Accordingly, each measured value of flow rate q has a different value of λ and this difference must be accounted for in each reported measurement. In other words, applying the equation of the line as a least square approximation to a linear curve will only provide an average value for $B = \delta\lambda/(2\pi)$. So, therefore, using the QFFM, each measured data point must be adjusted for the appropriate value of λ in order to accurately extrapolate the measured data in the incompressible fluid (water) to the extrapolated data for the compressible fluid (air). When this fine adjustment is made for each measured value, the correlations for measured and extrapolated data are superimposable.

Akinetic-Type Friction Factor-Dimensionless Permeability

In Figure 4A, we show a comparison of the dimensionless permeability in both water and air over the same range of pressure drops of 1 to 100 psi.

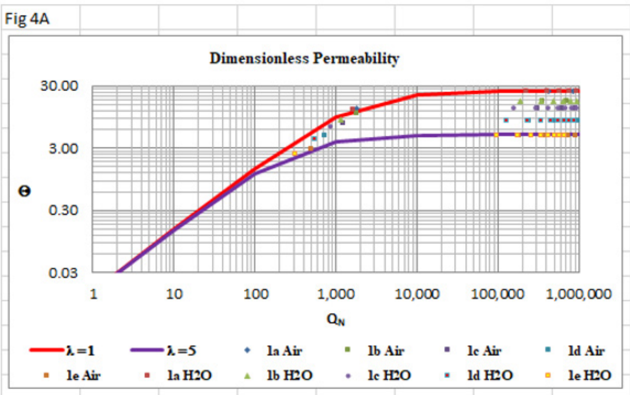

Figure 4A

In Figure 4A is shown the impact of the roughness coefficient (dimple depth) for each of the samples. For comparison purposes, the lines for λ = 1 and 5 are shown. Note that the samples all fall within this range of values for λ. This term is a second level kinetic-type friction factor which enables a precise determination of the impact of the roughness coefficient (depth of the dimples) on a golf ball manifested in the values of λ. Note that at low values of the Quinn number, $Q_N = dRe_m$, the term on the abscissa, all sample lines collapse onto a single line because the roughness of the particle surface is buried beneath the viscous boundary layer. Only when the value of Q_N is high enough to sufficiently deplete the boundary layer, does the roughness punch through the ever-declining boundary layer and manifest as values of l . Thus, at the higher values of Q_N, the differences in surface roughness of the golf balls are easily quantifiable which differentiates between the golf balls based upon their dept and frequency of dimples.

A Fluid Drag-Type Friction Factor-Quinn's Law of Fluid Dynamics in Closed Conduits

In Figure 5A, we show the QFFM friction factor in both water and air over the same range of pressure drops of 1 to 100 psi.

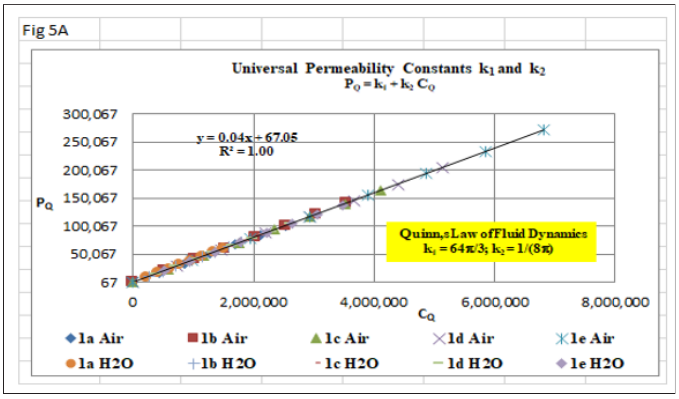

Figure 5A

In Figure 5A is shown the QFFM friction factor $P_Q = f_V/r_h$. This is a unique friction factor which is a fluid drag-type friction factor and is, therefore, normalized for fluid drag (r_h). Note that all measured conduits fall on this same straight line which confirms the universality of the constants k_1 and k_2. This is because the term on the abscissa of this plot, $C_Q = dlRe_m$, which we call the fluid current, is normalized for all variables involved in the kinetic term of the pressure flow relationship. Thus, packed conduits having different porosities and roughness all collapse onto the same straight line. Accordingly, this relationship is now termed "Quinn's Law of Fluid Dynamics in Closed Conduits" and identifies the values of the universal constants k_1 and k_2.

A Laminar Residual-Type Friction Factor-the Ultimate Residual Friction Factor

The QFFM friction factor outlined above is not a totally "residual" friction factor since both universal constants k_1 and k_2 have the universal constant p embedded. By residual we mean the remainder, representing the driving force term (pressure drop DP) in the pressure flow relationship, when the impact of all the terms in the relationship has been accounted for. In other words, if we were to define a fourth level friction factor P_Q^0 by normalizing for the universal constant (π/3) in the viscous term, we would identify the residual value of 64, approximately, i.e., $P_Q^0 = 3(P_Q - k_2 C_Q)/\pi = 64$. This value of 64 is recognizable as the value for the friction factor for laminar flow (low value of the Reynolds number) of conventional wisdom, found in most text books. Since the concept of a friction factor, however, is a mathematical construct, and, therefore, a man-made entity which has no basis whatsoever in Nature and is only relevant when grounded by experiment, the conventional value of 64 represents the entity $r_h^3 = 4^3 = 64$ which is the value for the volume of free space occupied by the viscous boundary layer when the fluid is at rest ($q = 0$). In other words, it represents a control volume of fluid when that fluid is at rest, in the mathematical expression for the pressure flow relationship which renders a correlation between mathematics and the dictates of the Laws of Nature which can be grounded/validated by experiment, such as has been accomplished in the unique case of the QFFM.

The Turbulent Tipping Point (TTP)

In Figure 6A, we show the TTP in both water and air for all 5 conduits in this study. We point out that the TTP is identical in both fluids.

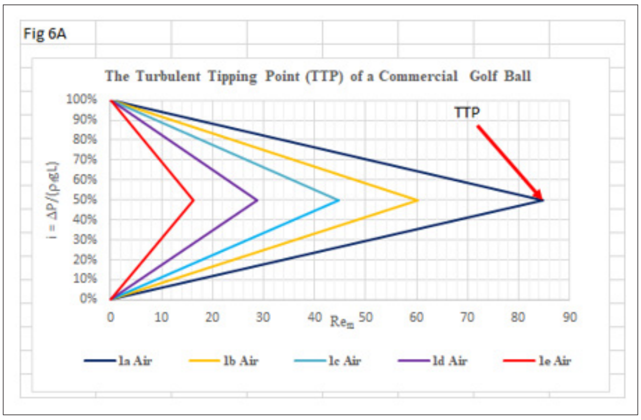

Figure 6A

In Figure 6A is shown the TTP for each sample as a function of the Reynolds number. Note that as the roughness coefficient increases, the TTP value of the Reynolds number decreases. The TTP is that precise point in the pressure flow relationship when the viscous and kinetic contributions to hydraulic gradient are identical (50%). As shown in Table 1A, the TTP in both water and air occurs at the same value of the Reynolds number. As can be seen from the plot, at the critical value of $C_{Q\text{-}C} = \delta\lambda Re_m = 1{,}686$, representing the TTP of fluid dynamics in closed conduits, dimensionless permeability is related to wall-effect as a reciprocal power function, i.e., $\Theta_C = 4\pi/\lambda$. Similarly, it can be shown that at the value $C_{Q\text{-}C} = 1{,}686$, the critical normalized pressure parameter $P_{Q\text{-}c} = 2k_1$. Thus, we can now add three new benchmarks to the portfolio of important fluid dynamic markers which define the TTP, i.e., $C_{Q\text{-}c} = 1686$, $\Theta_C = 4\pi/\lambda$ and $P_{Q\text{-}c} = 2k_1$

Validation

We now display our validation of the QFFM by using the results of our actual measurements. In Table 1C is shown the actual measurements we made. The first conduit was 20 feet in length ($L = 664$ cm) and was filled with 151 golf balls, $n_p = 151$. The second conduit was 21.5 inches in length ($L = 54.61$cm) and contained 13 golf balls, $n_p = 13$.

Table 1C																				
Sample	η	ρ_f	D	L	d_p	n_p	k	ρ_f	ε_B	d_e	Ratio	δ	λ	ω	T	t_d	TTP	TTP	A	B
ID								Δ_p	$(1-n_p/n_{pq})$	d_e	D	1	$1+V_m$	Ω	2π	$\Omega L d_e \varepsilon_B \rho_f$	$\Omega Re_{m\text{-}c}$	$Re_{m\text{-}c}$	$4\pi r_h^3$	Ω
Golf Ball								n_{pq}		abs(ρ_f)	d_p	ε_B^3		8π	ω	η	$C_{Q\text{-}C}$		3	2π
HQC	poise	gcm^{-3}	cm	cm	cm	none	cm	none	none	cm	none	none	none	rad/sec	sec	sec	none	none	none	none
H2O				20'																
np 151	0.010000	1.000000	4.40	664	4.27	151	0.E+00	0.6098	0.3902	7.002	1.03	16.84	2.500	1.67	4	7,633,305	1,686	40	268.19	6.70
				21.5'																
np 13	0.000183	0.001290	4.40	54.61	4.27	13	0.E+00	0.6382	0.3618	6.691	1.03	21.12	2.400	2.02	3	47,224	1,686	33	268.19	8.06

As shown in Table 1C, there is a small difference in the value of the HQC for the conduits under study. This is due to the small difference in the external porosity of each packed conduit.

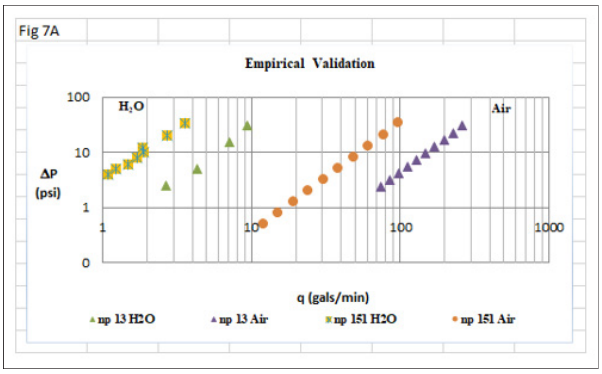

Figure 7A

In Figure 7A is shown our measured results in water as well as our extrapolated values in air.

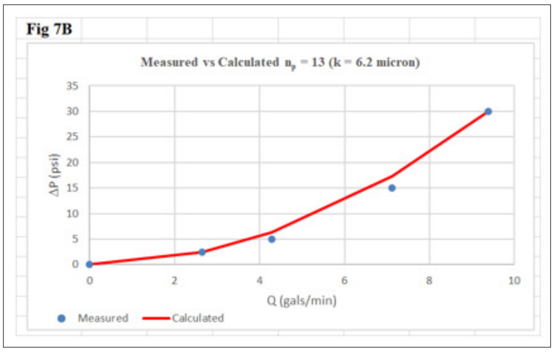

Figure 7B

In Figure 7B is shown a correlation between our measured and calculated values for the conduit containing 13 golf balls. Note that the best fit between the data was at a value of k = 6.2 micron. In other words, this result indicates that the golf balls had a dimple depth of 6.2 microns.

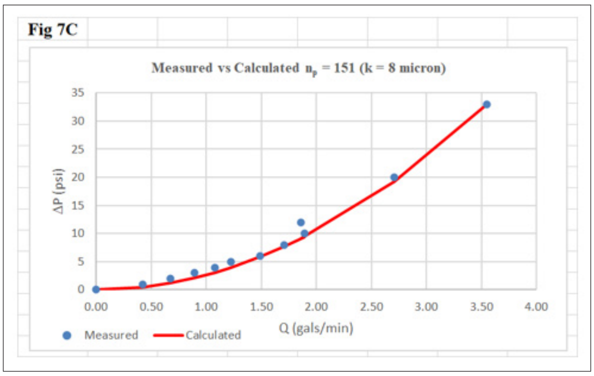

Figure 7C

In Figure 7C is shown a correlation between our measured and calculated values for the conduit containing 151 golf balls. Note that the best fit between the data was at a value of k = 8 micron. In other words, this result indicates that the golf balls had a dimple depth of 8 microns.

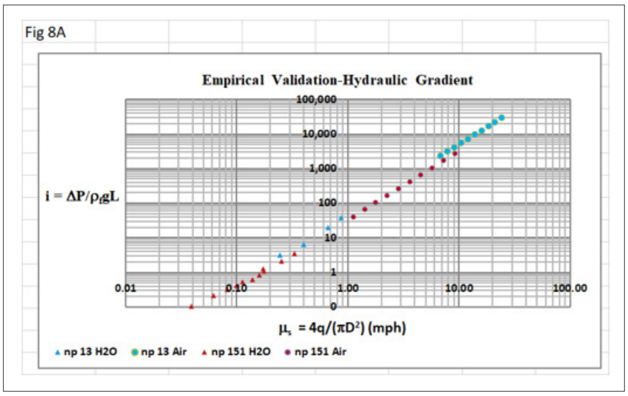

Figure 8A

In Figure 8A is shown the hydraulic gradient for both measured conduits. Note that the hydraulic gradient for both conduits is identical in water and air.

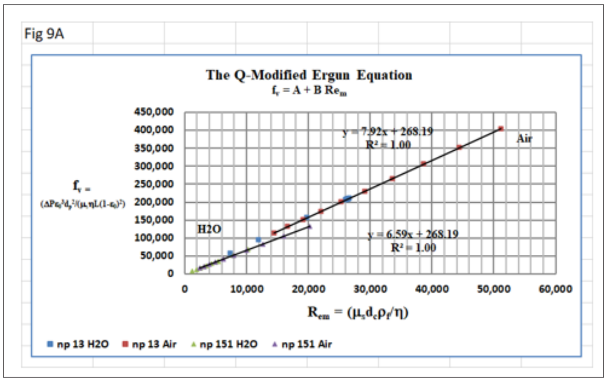

Figure 9A

In Figure 9A is shown the Q modified Ergun coefficients A and B for the two packed conduits under study. Note that both conduits have the same value for the line intercept A but slightly different values for the line slope B. This is because they have slightly different values for external porosity.

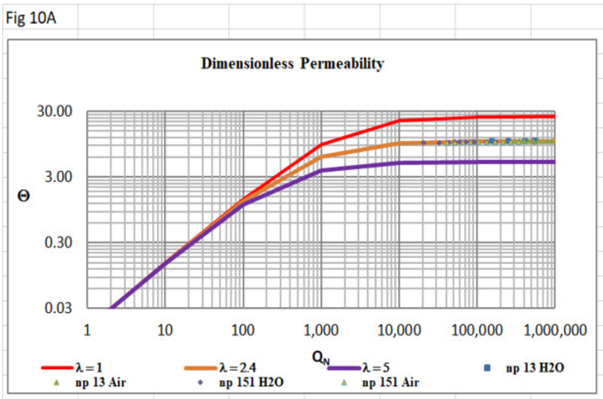

Figure 10A

In Figure 10A is shown the dimensionless permeability for both conduits. Note that both conduits have similar values for l which indicates that they have similar dimples on the ball surfaces.

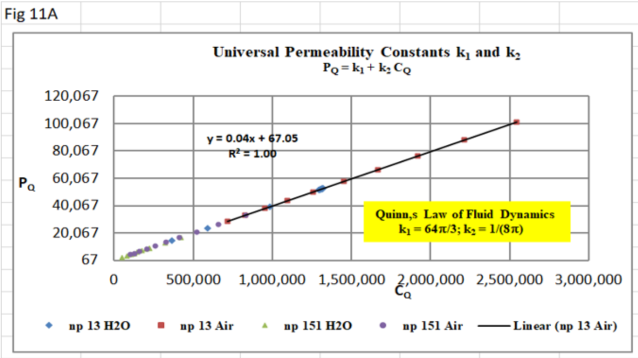

Figure 11A

In Figure 11A is shown the values for the universal constants k_1 and k_2. Note that all data points fall on the same straight line.

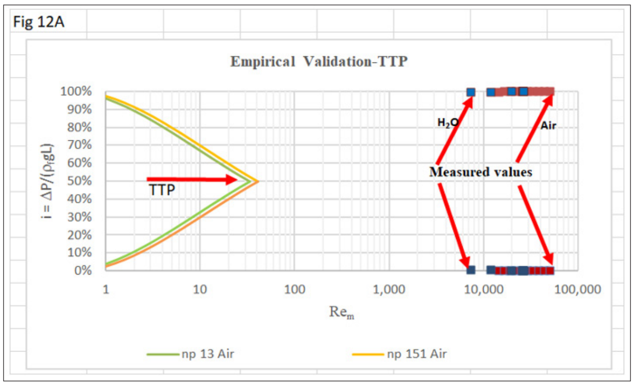

Figure 12A

In Figure 12A is shown the TTP for the two conduits in our study. Note that our pressure drop measurements were taken in the fully turbulent region of the flow regime ($Re_m > 5{,}000$). This is the region of the flow regime where roughness manifests due to the disappearance of the viscous boundary layer as fluid rotation and turbulence increases. Note that the TTP for these two conduits is at a Reynolds number of less than 50.

Finally, we show the velocity streamlines of our example of the packed conduit containing 151 golf balls.

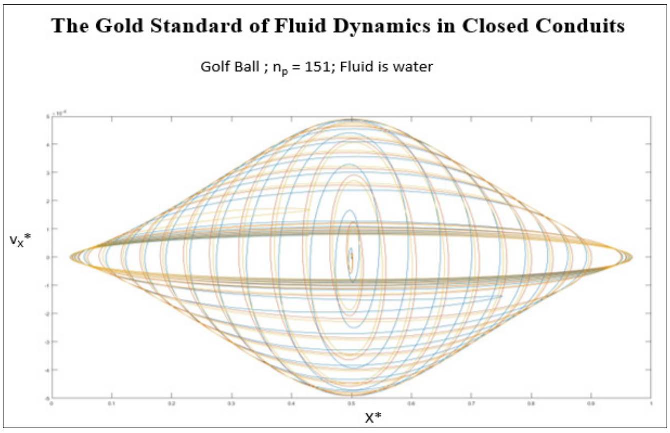

Figure 13A

Figure 13A shows the fluid velocity streamlines of our example of 151 golf balls with water as fluid. This plot is generated using the QFFM in the engineering program language of MathLabTM. We can see the transition from laminar flow to fully turbulent flow as the fluid accelerates from rest to the maximum flow rate, in this case circa 30 psi. The streamlines begin with a parabolic shape in laminar flow and end as almost flat curves at maximum speed. We show this plot in water, not air, because the streamlines in air would be too close together to see clearly. In other words, water provides a slow-motion snapshot of the golf ball flight as compared to air.

Conclusions

In this paper, the 12 principles of fluid dynamics in closed conduits are defined and documented. In addition, as a worked example, the aerodynamic performance of a golf ball is specified. This worked example has been accomplished by making permeability measurements in water and extrapolating them into the fluid air using the QFFM. As far as we know, this has never been accomplished before. This analysis is made possible by the dictates of the Laws of Nature, which teaches that it does not matter which one of the two media types present, particles or fluid, is stationary and which one is in motion. Accordingly, we are able to take measurements of a conduit filled with golf balls in water and by extrapolation, demonstrate a ball in aerodynamic flight through air which remains at STP at all speeds, which is the case on a golf course. The conclusions drawn from this paper may be stated as the 12 principles of fluid dynamics in closed conduits which are:

- Hypothetical Q Channel (HQC); $d_c = d_p/|p_f|$ (cm).
- Q time constant; $t_Q = \delta\lambda L d_c \varepsilon_t p_f/\eta$ (sec).
- Fluid/particle rotation; $\omega = \delta\lambda/(8\pi)$ (radians/sec).
- Period of the motion; $T = 2\pi/\omega$ (sec)
- Permeability; $\Delta P = aq + bq^2$
- Hydraulic gradient; $i = \Delta P/(p_f gL)$ (dimensionless)
- Viscous type friction factor; $f_v = A + BRe_m$ (dimensionless)
- Kinetic type friction factor; $Q = Q_N/P_Q$ (dimensionless)
- Drag normalized friction factor; $P_Q = k_1 + k_1\ C_Q$ (dimensionless)
- Residual laminar friction factor ff_r ; $\Theta_Q^0 = 3(P_Q - k_2 C_Q)/\pi = 64$ (dimensionless)
- Turbulent tipping point (TTP); $Q_c = 4\pi/\lambda = 1{,}868$ (C_Q)
- Fluid velocity streamlines $v_x^* = v_x/\mu_f$ (cm/sec²)

References

1. Darcy H (1856) Les Fontaines Publiques DE LA Ville de Dijon. Victor Dalmont, Paris, France, Bnf Gallica's https://gallica.bnf.fr/ark:/12148/bpt6k624312.image.
2. de Azevedo HS, Franco MM, Morales REM, Franco AT, Junqueira SLM, et al. (2009) Flow pattern and Friction Measurements of Turbulent Flow in Corrugated Pipes. 20th International Congress of Mechanical Engineering, November 15-20.
3. Baker MJ, Tabor GR (2010) Computational analysis of transitional air flow through packed columns of spheres using the finite volume technique. School of Engineering, Mathematics and Physical Sciences (SEMPS), Harrison Building, University of Exeter, North Park Road, Exeter, EX4 4QF, UK 34: 878-885.
4. Erdim E, Algiray O, Demir I (2015) A revisit of pressure drop-flow rate correlations for packed beds of spheres. Powder Technology 283: 488-504.
5. Dukhan N, Bagci O, Ozdemir M (2014) Experimental flow in various porous media and reconciliation of Forchheimer and Ergun relations. Experimental Thermal and Fluid Science 57: 425-433.
6. Anspach JA, Maloney TD, Colon LA (2007) Ultrahigh-pressure liquid chromatography using a 1-mm id column

packed with 1.5-m porous particles. J Sep. Sci 30: 1207-1213.
7. Zhong W, Xu K, Li X, Liao Y, Tao G, et al. (2016) Determination of pressure drop for air flow through sintered metal porous media using a modified Ergun equation. Advanced Powdered Technology 27.
8. Tian FY, Huang LF, Fan L, Qian JL (2016) Pressure drop in a packed bed with sintered ore particles as applied to sinter coolers with a novel vertically arranged design for waste heat recovery. Applied Physics and Engineering 17: 89-100.
9. Mayerhofer M, Govaerts J, Parmentier N, Jeanmart H, Helsen L (2011) Experimental investigation of pressure drop in packed beds of irregular shaped wood particles. Powder Technology 205: 30-35.
10. Pesic R, Radoicic TK, Boskovic-Vragolovic N, Arsenijevic Z, Grbavcici Z (2015) Pressure drop in Packed beds of spherical particles at ambient and elevated temperatures. Chem. Ind. Chem. Eng Q 21: 419-427.
11. Abidzaid ZT, Kareem NO, Abbass MN (2010) Modified Equations for Water Flow through Packed Bed for different types of packing systems. Iraqi Journal of Engineering 6: 60-69.
12. Mirmanto (2013) Developing Flow Pressure Drop and Friction Factor of Water in Copper Microchannels. Journal of Mechanics Engineering and Automation 3: 641-649.
13. Carpinlioglu MO, Ozahi E (2008) A simplified correlation for fixed bed pressure drop. Powder Technology 187: 94-101.
14. Yang P, McCabe T, Pursch M (2011) Practical comparison of LC columns packed with different superficially porous particles for the separation of small molecules and medium size natural products. J. Sep. Sci 34: 2975-2982.
15. Khayamyan S, Lundstrom TS, Hellstrom JUG, Gren P, Lycksam H (2017) Measurement of Transitional and Turbulent Flow in a Randomly Packed Bed of Spheres with Particle Image Velocimetry. Transp. Porous Media116: 413-431.
16. Sletfjerding E, Gudmundsson J, Sjoeen K (1998) Flow Experiments with High Pressure Natural Gas in Coated and Plain Pipes. PSIG Annual Meeting 28-30.
17. Langeiandsvik LI, Postvolt W, Aarhus B, Kaste KK (2001) Accurate Calculation of Pipeline Transport Capacity. Personal Communication, Gassco, AS https://www.iapg.org.ar/WGC09/admin/archivosNew/Special%20Projects/4.%20IGU%20Best%20Practices/4.%20IGU%20Best%20Practices%20FINAL%20-%20CD%20contents/3.%20Transmission%20-%20Accurate%20calculation%20of%20pipeline%20transport%20capacity.pdf.
18. Stephano De (2008) Characteristics of Superficially-Porous Silica Particles for Fast HPLC: Some Performance Comparisons with Sub-2-μm Particles. Journal of Chromatographic Science 46.
19. Pereira L (2012) What Pressure to Expect from the Thermo Scientific Accucore HPLC Columns? Thermo Scientific Literature Technical Note 20542.
20. Van Lopik JH, Snoeijers R, Van Dooren TCGW, Raoof A, Schotting RJ (2017) The Effect of Grain Size Distribution on Nonlinear Flow Behavior in Sandy Porous Media. Trahs Porous Media 120: 37-66.
21. Li Z, Wan J, Huang K, Chang W, He Y (2017) Effects of particle diameter on flow characteristics in sand columns. International Journal of Heat and Mass Transfer 104: 533-536.
22. Nikitin M, Quinn, Pashchenko D (2025) Flow through packed beds: Experimental and numerical validation of the Quinn fluid flow model. Phys Fluids 37: 084113.
23. Papkov V, Quinn HM, Pashchenko D (2025) Flow through randomly packed beds of rough particles: Model prediction and experimental validation. Phys. Fluids 37: 103318.
24. Quinn HM, Pashchenko D (2026) A new semi-empirical model for pressure drop prediction in a packed bed of smooth and rough particles: Derivation and verification Phys. Fluids 38: 016101.
25. Quinn HM (2025) A Comparison of Sir Osborne Reynold's 1883 Seminal Paper and the QFFM; A Hand in Glove Reconciliation. European Journal of Applied Sciences 13: 71-92.
26. (1939) Laws of Flow in Rough Pipes NASA TM 1292.
27. Giddings JC (1965) Dynamics of Chromatography, Part I, Principles and Theory, Marcel Dekker, Inc. New York https://ia902901.us.archive.org/9/items/in.ernet.dli.2015.147899/2015.147899.Dynamics-Of-Chromatography-Part-1-Principles-And-Theory.pdf.
28. Farkas T, Zhong G, Guiochon G (1999) Validity of Darcy's law at low flow-rates in liquid chromatography. Journal of Chromatography An 849: 35-43.
29. McKeon BJ, Zagarola MV, Smits AJ (2005) A new friction factor relationship for fully developed pipe flow. Journal of Fluid Mechanics 538: 429-443.